Contribuciones del Instituto Nacional de Investigaciones Nucleares al avance de la Ciencia y la Tecnología en México

Edición conmemorativa 2010

Chapter 13

Plasma applications in materials modification, environment and medicine

English version of:

Capítulo 13

Aplicaciones de los plasmas en la modificación de materiales, en medio ambiente y en medicina

Published originally in the book:

Contribuciones del Instituto Nacional de Investigaciones Nucleares al Avance de la Ciencia y la Tecnología en México
Edición Conmemorativa 2010

Translation: Samuel Barocio Delgado

Plasma applications in materials modification, environment and medicine

R. López-Callejas, R. Valencia-Alvarado, A. Mercado-Cabrera, R. Peña-Eguiluz,
A. E. Muñoz-Castro, S. R. Barocio, B. G. Rodríguez-Méndez,
Department of Physics, ININ

A.de la Piedad Beneitez
Toluca Institute of Technology

regulo.lopez@inin.gob.mx

Abstract
Research work carried out at ININ Plasma Physics Laboratory concerning plasma applications has been focused on: a) ion implantation in stainless steels, titanium and aluminium, b) elimination of micro-organisms in liquids, c) bacterial suppression in biological media and dental surfaces and d) SO_2 decomposition by corona discharges and NO_X, H_2S decomposition by dielectric barrier discharges.

1. Nitrogen and oxygen ion implantation in materials

Some recent advances in materials treatment by means of plasma immersion ion implantation (PIII and PSII) are depicted in figure 1. A negative high voltage pulse between -1 and -300 kV, 1-200 ms long, is applied at a frequency between 10 and 1000 Hz to a sample immerse in a plasma. As soon as the sample becomes biased positive ions in the plasma are accelerated towards and implanted in it. Three distinct experimental PIII facilities are being developed at ININ Plasma Physics Laboratory (ININ-PPL): a) a toroidal 17 litre reactor (figure 2a) operating on DC as well as RF plasma discharges, b) a cylindrical 42 litre reactor (figure 2b) for DC plasmas and, c) a cylindrical 35 litre reactor for RF plasmas (figure 2c). Current experiments are being conducted on stainless steel, titanium and aluminium samples.

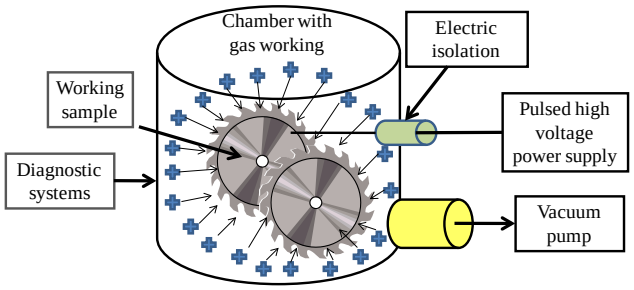

Figure 1. Plasma ion implantation process

1.1 Stainless steels

Drills and burs are essential dental instruments (figure 3b). Their frequent contact with the aggressive mouth environment, where saliva and bacteria corrode them [2], demands special tool treatments intended to enhance their tolerance to chemical attack and friction wear. One of the more attractive characteristics of the plasma immersion ion implantation

(PIII) treatment of objects with complex topology (figure 3a) is not requiring the rotation and/or translation of the target piece. Such objects have been biased at ~ -5 kV by means of a pulse modulator at ~1 kHz frequencies resulting in ~5-100 μs wavelength pulses which enable to control the piece temperature that results from the ion bombardment. Thus, a nitrogen plasma density of ~10^{16} particles/m^3 lead to a homogenous ~5-30 μm implanted thickness after a 3-4 hour treatment period.

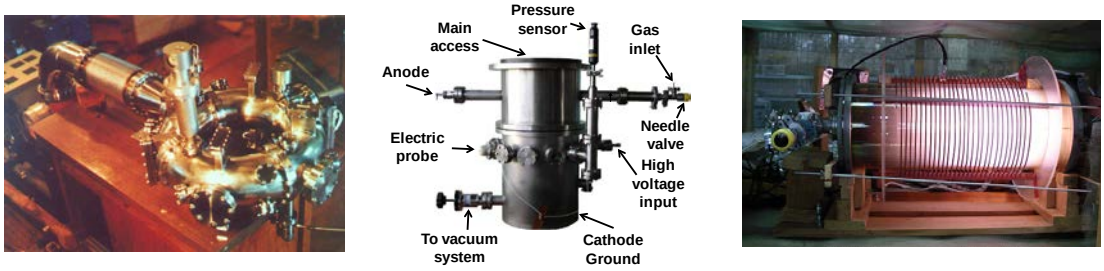

a b c

Figure 2. Plasma discharge reactors: a) toroidal, b) cylindrical DC and c) cylindrical RF.

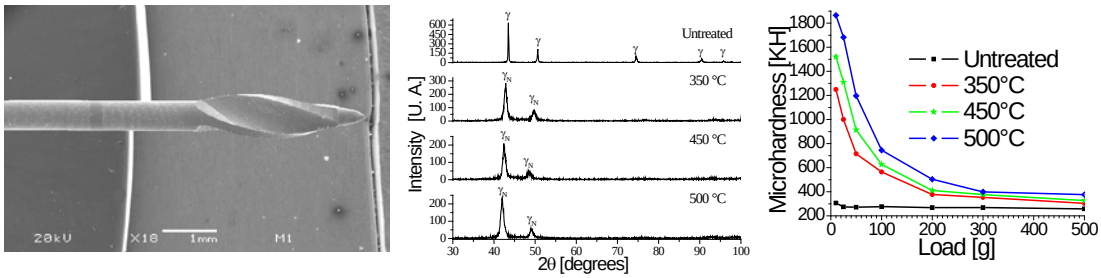

a b c

Figure 3. a) Micrography of a typical dental drill, b) DRX spectra and c) Microhardness

PIII treated drills have been analysed by means of the scanning electronic microscope (SEM) yielding micrographies of the implanted material. Elemental analysis of these drills has been provided by x ray diffraction (XRD) revealing the nitrogen content of the modified layer of each piece. The drill atomic percentage proves that the diffusion of nitrogen is favoured by temperature increase. Nitrogen shows a tendency to expand the lattice, facilitating the inclusion of new atoms in it, provided that the sample temperature does not exceed the precipitation temperature of the steel components. According to the XRD analysis the nitrided layer displays an iron crystalline structure in the γ_N (expanded austenite) phase when the piece has been implanted between 350 °C and 500 °C [2, 3]. Additional evaluation of the treatment was provided by Knoop microhardness tests which were conducted along a longitudinal section of each drill. The best hardness values were achieved at the highest bias temperatures (figure 3c) albeit with a sharp tendency to decrease with the applied load according to the nitrided layer thickness. The surface hardness increase can be attributable to the lattice expansion created by the inclusion of nitrogen. This phenomenon is closely related to wear resistance enhancement [2-5].

1.2 Biomaterials

On the basis of body contact form and duration, biomaterials are classified as either temporal or permanent as well as either internal or outward. From a functional point of view, biomaterials can be destined to support, diagnosis or treatment. As they restore body functions, it is relevant to understand the relationship existing between living tissue and organs on the one hand, and the properties, functions and structures of biomaterials on the other hand. In particular, the success of a biomaterial implant depends on material properties and biocompatibility, the health condition of the recipient and surgical skill.

The quest for materials with a high resistance to wear and the development of surface modification technologies command a high degree of attention in the scientific community [6-11], especially with respect to the so called load implants. The ideal materials for hard tissue substitution prosthetics should fulfil the following properties:

- Biocompatible chemical composition
- Excellent tolerance to internal human body corrosion
- High wear resistance and low residual production

To these, it should be added enough bioactivity as to ensure the osteointegrability of the implant, indispensable for the direct cementing of artificial bones, joints and dental implants avoiding adverse rejection reactions. Titanium and its alloys display outstanding mechanical qualities such as its high tolerance to corrosion although some poor surface characteristics have limited their applications [7, 8]. Such tolerance depends on the existence of a 2 to 7 nm thick firmly adhered oxide patina [12, 13] produced by the contact with the atmosphere. The performance of titanium in surgical implants can be assessed from its response to corrosive species existing in the human body fluids. Actually, titanium by itself is not a biocompatible material. When absorbed by the body, it can cause serious problems such as osteogenic differentiation in the human medulla cells [14]. Thus, titanium must be previously processed in order to either protect or enhance its natural oxide layer.

During the last decade divers methods have been tested in order to improve the surface qualities of titanium, among others, plasma aspersion coating [6-10] or nitrogen and oxygen ion implantation by plasma immersion carried out at ININ PPL [15-19] as to:

- Developing nitrided layers on the titanium surface increasing its hardness and wear resistance.
- Increasing titanium biocompatibility by adding oxide layers in the rutile phase.

Results reveal the achievement of titanium dioxide (TiO_2) films in DC and RF plasmas, mainly in the rutile and anatase phases (figures 4a and 4b). Samples were previously treated in argon plasma with cleansing purposes. The results were characterised by means of XRD (figure 4a), Raman spectroscopy (figure 4b) and SEM (figure 4c). The former two indicated the presence of the rutile, and, eventually, the anatase phases. Micrographs of the cross section of the samples show an implantation depth between 3 and 6 μm. SEM images provide a measure of the grain and the degree of homogeneity achieved by the treatment. Microhardness tests indicate increases up to 500%.

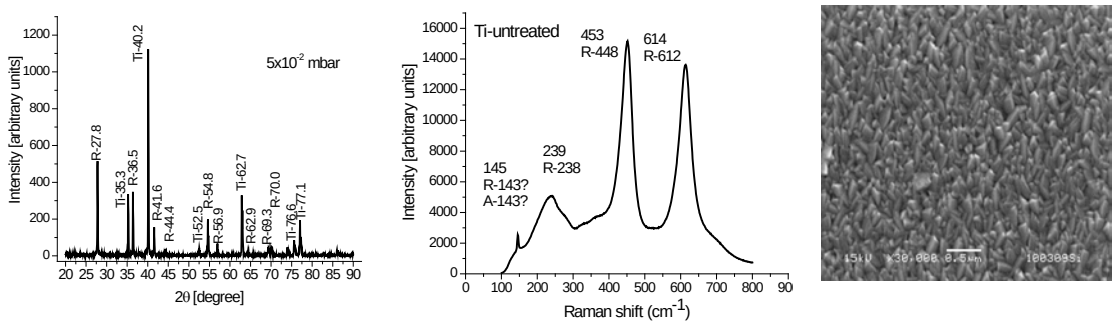

a b c

Figure 4. Experimental characterisation of the PIII processed samples: a) XRD typical spectrum, b) Raman spectroscopy diagnostic and c) SEM

1.3 Aluminium

A non ferrous metal, aluminium combines qualities highly appreciated in mechanical engineering like low mass density and high corrosion tolerance. Yet, its mechanical response is rather poor unless improved by alloying. By contrast, aluminium is a good electric conductor, readily machined and rather inexpensive, whereby it is second only to steel in the industrial demand. Aluminium is surrounded by a native oxide layer which lends it resistance to both corrosion and wear. Modifying aluminium composition by nitrogen implantation results in high surface hardness and enhanced friction and wear endurance.

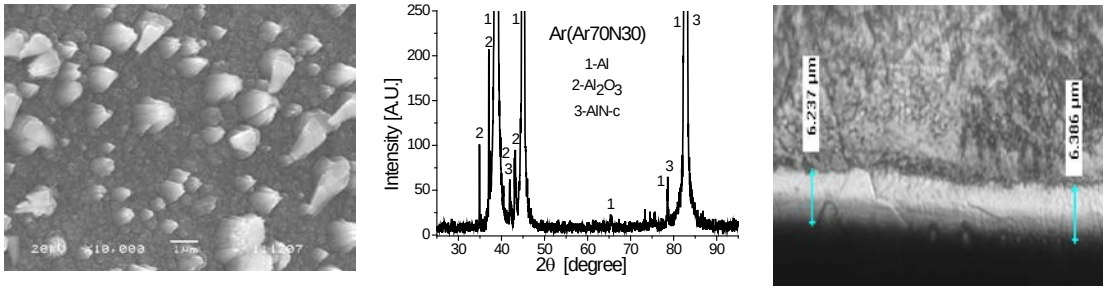

a b c

Figure 5. a) Micrograph of PIII treated aluminium simple. b) Diffractogramme and c) Cross sectional micrograph of the implanted layer

A considerable amount of experimentation at ININ-PPL has been dedicated to determine the optimal efficacy conditions for PIII aluminium nitriding [20] as well as the best technique for surface TiO_2 layer enhancement so to increase aluminium biocompatibility in the most economical way. Tribological improvement has been accomplished by PIII in pure nitrogen plasma as well as using nitrogen-argon mixtures. The determinant role played by temperature in the PIII process has been established by identifying the optimal 300°C-500°C region by varying the voltage amplitude and width of the implantation pulse while maintaining a constant 2×10^{-2} Torr gas pressure conducive to a 10^{16} particles per m^3 plasma density. Figure 5a exhibits the SEM outcome after the treatment. Optimal Vickers microhardness at a 100 gf load was achieved in 70% nitrogen 30% argon mixture plasmas with 400°C sample temperature and pulse width-voltage values between 0.27 and 0.3 V·µs. Coincidentally, the samples thus treated present the maximal rugosity values, which are ideal to ensure adherence to live human cells: a fundamental requirement for biomaterials.

Most treated samples are found in the cubic phase and, to a lesser degree, in the hexagonal one (figure 5b). The nitrogen implanted layer typical depth can be seen in figure 5c as a cross section.

2. Micro-organism elimination in liquids

The most common method of water disinfection is chemical application which unavoidably leads to the formation of by products hazardous to public health. For instance, the use of dichlorine (Cl_2), sodium hypochlorite (NaOCl) or chlorine dioxide (ClO_2) generates compounds such as chlorofluorocarbons, perfluorinated compounds, chloramines, trihalomethanes and hypoclorous acid, among others [21]. Trihalomethanes in particular are known to inflict serious damage to liver, kidney and central nervous system, apart from being an active carcinogenic agent. Nevertheless, several electrotechnical water treatment technologies such as oxidation by ozone or electronic irradiation have shown promising results [22]. For instance, the electric discharges employed in ozone synthesis are a current industrial application of these technologies [23, 24] whose non thermal disinfection methods include:

- Injection of ozone, which is an allotropic form of oxygen that reacts keenly with the cell membrane of bacteria. Ozone is the product of corona or DBD plasma discharges.
- Pulsed corona discharges that generates free radicals lethal to micro-organisms and breaks down organic molecules, mainly by oxidation.
- Pulsed ultraviolet radiation which disintegrates the ADN of micro-organisms.
- Pulsed electric fields that disables cells by tearing at the membrane by electroporation

ININ-PPL is currently conducting two theoretical-experimental programmes aimed at water disinfection: the generation of pulsed corona discharges (PCD) and of dielectric barrier discharges (DBD) [25-27]. The first activity required the development of a PCD model, as an electronic circuit, including:

a) Static parameters determined by the physical characteristics of the environment.
b) Ionisation and avalanche expansion mechanisms (e.g., streamers) following a pre-breaking current resulting from changes in the capacitance and resistance of the discharge.
c) Electric breakdown in water characterised by the presence of a highly conductive channel with a net current flux represented by a saturation resistance and an inductance.

This model can predict the behaviour of a particular discharge which, in turn, suggests the instrumentation characteristics for a possible experimental generation of a PCD.

Arcing free discharge generation has been achieved by the design and construction of a power supply generating high voltage pulses up to 30 kV, 1-30 μs long, at a 0 to 1000 Hz repetition rate. Both the pulse width and frequency are adjusted by means of a time clock. The power supply was coupled to either of the two reactors where *Escherichia coli* bacteria are eliminated, namely:

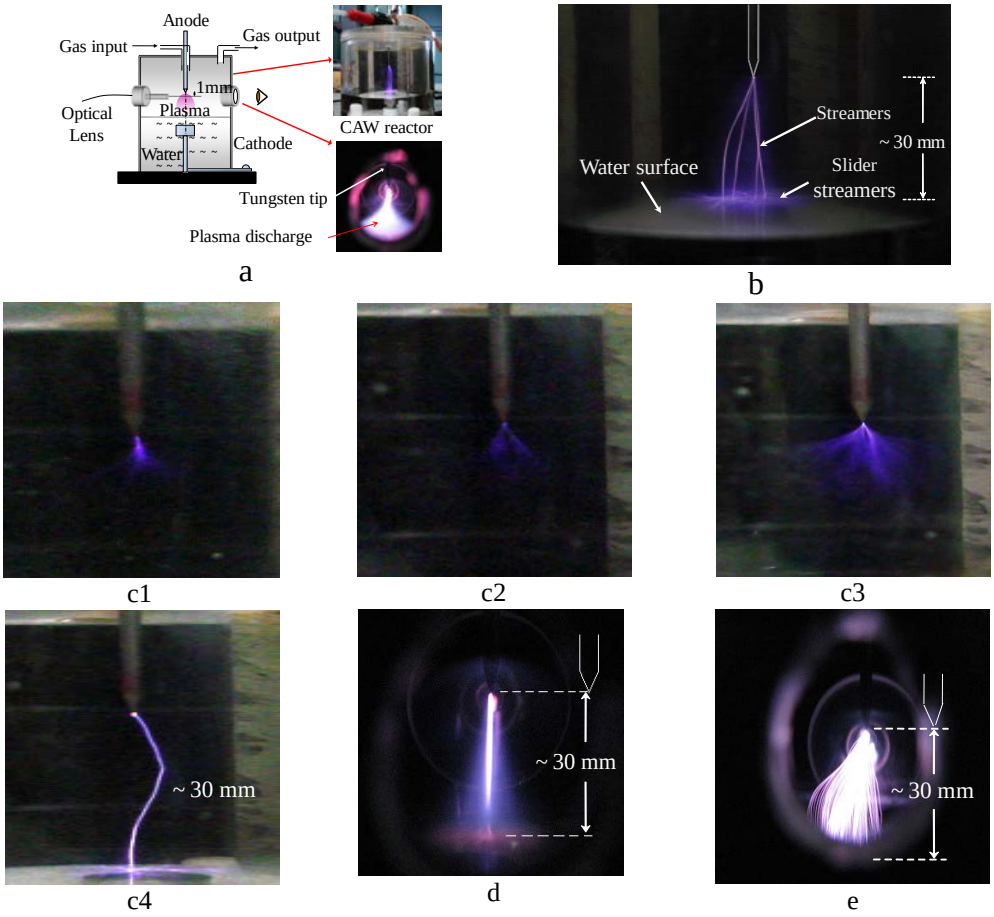

Figure 6. Generation of plasma discharges in point to plane reactor: a) Reactor scheme, b) Experimental discharge, c) Discharge evolution at different voltages: c1) 4 kV, c2) 6 kV, c3) 10 kV y c4) 12 kV. Discharge on water in: d) helium and e) argon.

a) A first reactor in point to plane configuration (figure 6.a) generates the discharge between the electrode point and the water surface delivering energetic electrons, UV radiation, active chemical species and shock waves. The electrons collide with the water molecules which result dissociated generating a great many free radicals like OH, H, HO_2, and other species such as ozone (O_3). The latter is dissolved into the water forming hydrogen peroxide (H_2O_2). The reactor is structured as a methyl-methacrylate 0.084 m tall cylindrical container with a 0.066 m diameter. The positive electrode is shaped as a tungsten needle, 0.0015 m in diameter, tapered off at a 40° angle and movable with respect to the negative electrode. The latter consists of a stainless steel circular plate of a 0.007 m diameter, which is submerged into the water. As shown in the photograph sequence of figure 6, an increasing bias voltage results in the formation of several simultaneous conduction channels which, once reaching the water surface, become radially distributed giving place to the so-called sliding expansion of the electron avalanche [28]. These electrons propagate to the cathode plate as long as the voltage is kept constant. The experimental evidence indicates that the most influential factor in the shape and number of conduction

channels in the point to plane configuration is the amplitude and width of the voltage supply.

b) The second reactor consists of a tungsten filament (anode) encased in ceramic concentric to a 0.3 m long stainless steel cylindrical chamber (cathode) of 0.0127 m diameter, namely 0.000152 m^3 in volume. The chamber is completed with two nylamid lids, as shown in figure 7a where high voltage pulses are applied to the electrodes by means of two connectors. The design includes an inlet for the injection of oxygen facilitating the discharge and enhancing the production of chemical species. Figure 7b display images of the DBD discharges in helium and argon.

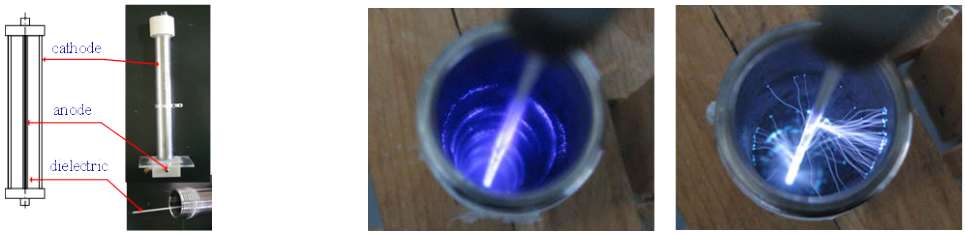

a b

Figure 7. Generation of plasma discharges in DBD reactor: a) Reactor structure for plasma discharges in water; b) Physical characteristics of a DBPD in: helium (left) and argon (right)

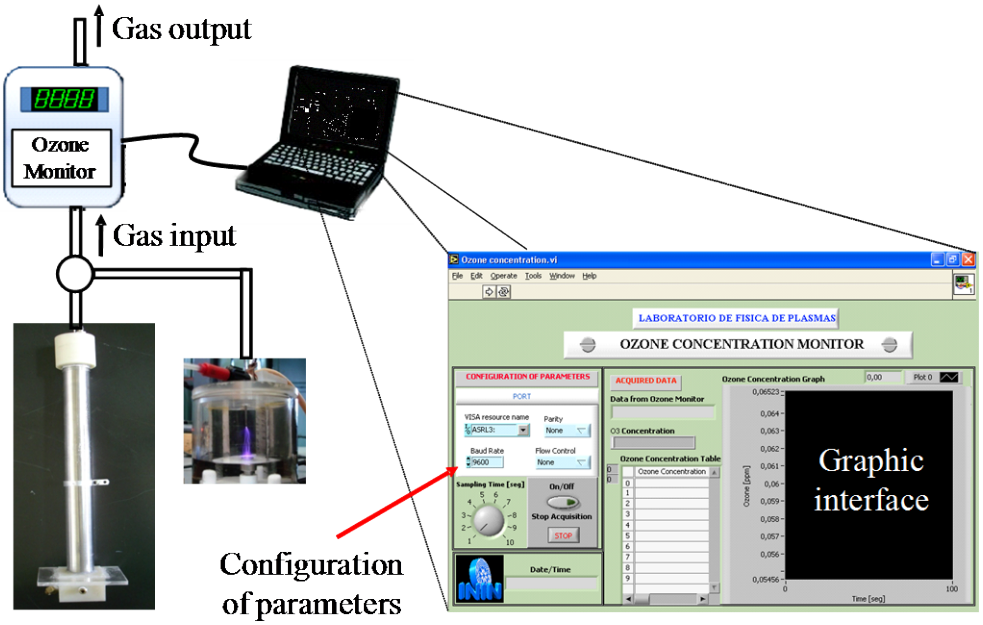

Figure 8. Diagramme of the ozone determination system on LabView

The presence of the chemical species produced by the discharge has been observed *in situ* at each reactor by means of UV absorption and optical emission spectroscopy (OES) at room pressure. Thus the genesis of highly oxidising species such as hydroxyl radicals OH and O_3 as a function of the discharge parameters is quantitatively and qualitatively

examined. Ozone determination demanded the development of a data visualisation and acquisition on the basis of a LabView™ platform (figure 8).

The optimal experimental conditions for E. Coli elimination are found to include a 25 kV bias pulse with 15 μs width at a 500 Hz repetition rate. The bacterial populations have been kept in 15 mL volumes of distilled water, the process having been accelerated by the injection of a 0.00833 L/s oxygen flow. Figure 9 present the bacteriologic outcome from the treated samples, in particular, when the initial concentration is around 5.31×10^{8} CFU/mL (colony forming units/millilitre). Clearly, the gradual elimination process depends on the treatment time ranging from 2 minutes (figure 9a) up to 27 minutes (figure 9f).

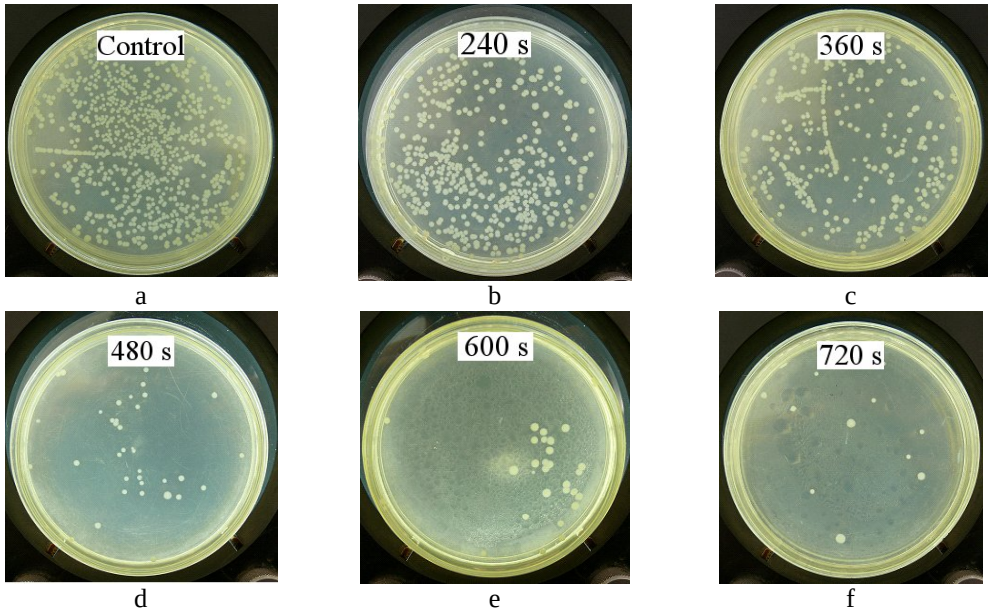

Figure 9. Bacteriologic analysis of CFUs of E. coli. a) Reference sample, b)-f) gradual elimination at several treatment times

3. Biological and medical plasma application

The antecedents of room pressure out of thermal equilibrium plasmas applied to biological media begin in 1964 when W. P. Menashi presented a patent request entitled 'Surface treatment' being finally approved in 1968 [29]. Ever since and in a gradual way, multiple works have been published around the world dealing with applications of such plasmas, whose ions and electrons are not in thermal equilibrium, like the suppression of micro-organisms on surfaces and biological media, the treatment of skin and mucous membranes or the sterilisation of surgical instruments, which constitute nowadays fields of the greatest interest [30-32]. One early work carried out at ININ-PPL comprised the design and construction of a low cost highly effective RF voltage signal power source at 13.54 MHz intended for room temperature electric discharges. This source was tested on especially developed discharge reactors [33]:

a) Plasma needle (figure 10a) structured from a central capillar electrode, 0.33 mm in diameter, encased in a ceramic material and protected by a 50 mm long dielectric capsule through which gas is injected to be ionised.

b) Dielectric free parallel plate reactor (figure 10b) whose electrodes are 80 mm diameter stainless steel discs separated by a 1 mm gap.
c) Parallel plate reactor (figure 10c) with similar characteristics to the previous one but endowed with a I mm deep Petri dish acting as dielectric between the plates 3mm apart.
d) Coaxial DBD (figure 10d), containing a central capillar electrode encased in dielectric material. The latter is constituted by 4 mm diameter glass spheres contained in a 30 mm long glass cylinder of 11 mm diameter wrapped in a copper mesh acting as the second electrode.

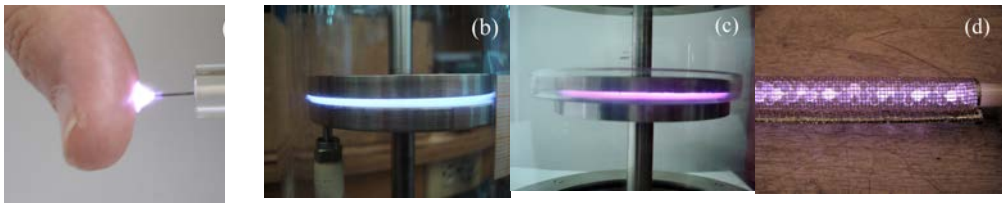

Figure 10. Reactor configuration: a) Plasma needle, b) Parallel plate without dielectric, c) Parallel plate with dielectric, d) Coaxial DBD

RF plasma needles [34] generate a small volume of glow plasma at the tip (figure 10a), which performs with extreme precision in the treatment of organic materials and surfaces at no risk of thermal or electric damage. Experimental tests of such a system conducted at ININ-PPL have followed the development of an electrical model of the discharge behaviour. The conditions of steady operation were then established and plasma temperature profiles were determined. Discharges were conducted in helium and argon as bearing gas in order to verify their effectiveness in medical applications [35]. Figure 10a exhibits the interaction of the plasma needle with live human skin.

The instrumentation developed for the micro-organism elimination tests using room temperature plasmas out of thermal equilibrium, is constituted by a specific RF signal generator supplying directly each discharge reactor so as to generate the right kind of active species to process previously characterised cultures [30-32].

3.1 Escherichia coli (E. coli) bacteria elimination by plasma needle

The methodology and tests of E. coli elimination were developed at the Microbiology Department of the University of Guadalajara, Mexico, on the basis of direct application of plasma on a small area inoculated with an initial 1.2×10^{7} (CFU/mL) bacteria concentration, characterised by the McFarland method. The concentration is indirectly determined from the sample absorbance by means of a spectrophotometer tuned to a 635 nm wavelength.

The needle experimentation took place in a 1.5 L/min helium flux at power supply between 22 and 40 W on the cultures. The treatment periods were conveniently programmed so as to register the mortality evolution in the colonies (figure 11). The resulting CFU survival curve of E. coli is presented in figure 11d. Typically, the total elimination at a 40 W power is achieved at 80 s of treatment whereby the total energy required is 3.6 kJ. Greater concentrations of active species, dependant on higher magnitudes of the applied voltage,

improve the effects on the micro-organisms. Therefore, the elimination is more effective at higher voltages with shorter exposure periods [36].

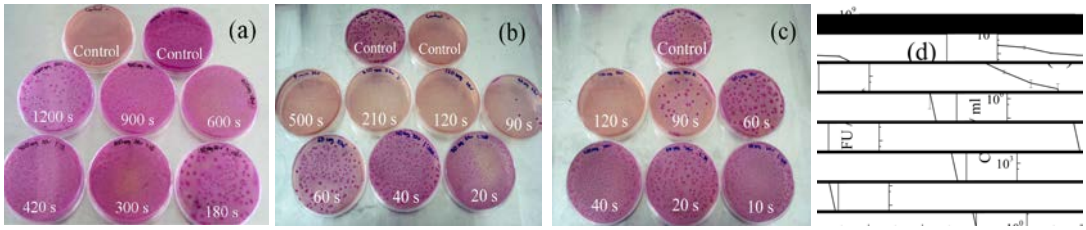

Figure 11. E. coli cultures from samples exposed to plasma needle for several periods at: a) 22 W, b) 30 W, c) 40 W. d) Evolution of surviving E. coli colonies at 40 W

3.2 Micro-organism elimination in a parallel plate DBD

The experimental methodology of the DBD micro-organism elimination (figure 10c) is based on the inoculation of sterile paper discs of 1 cm diameter with 20 μl of culture suspension, as shown in figure 12.a. The discs are placed in Petri dishes in the 2.5 mm gap between the DBD plates. The discharges are conducted in a 1.5 L/min helium flow at a 45 W power.

Two evaluation techniques have been applied:

a) The turbidimetric method establishes the incorporation of each one of the samples in a test tube containing 3 mL Bioxon urea, stirring as to homogenise the solution while liberating the bacterial content of the disc. Each test tube is incubated for 9 h at 35 °C for better development. The initial concentration was in the order of 1.5×108 CFU/mL. The surviving CFU concentrations of four distinct bacteria, namely, P. aeroginosa, S. cerevisiae, S. aureus and E. coli, are presented in figure 12b.

b) The potenciometic method consists in placing each inoculated paper in a test tube containing 5 mL of phenol red mixed with 0.75% glucose Merck Microbiology. The tube is then shaken so to accelerate the dilution of the bacterial content. After 7 h incubation at 35 °C, reductions in the pH levels are evidenced by a colour shift of the red phenol indicator.

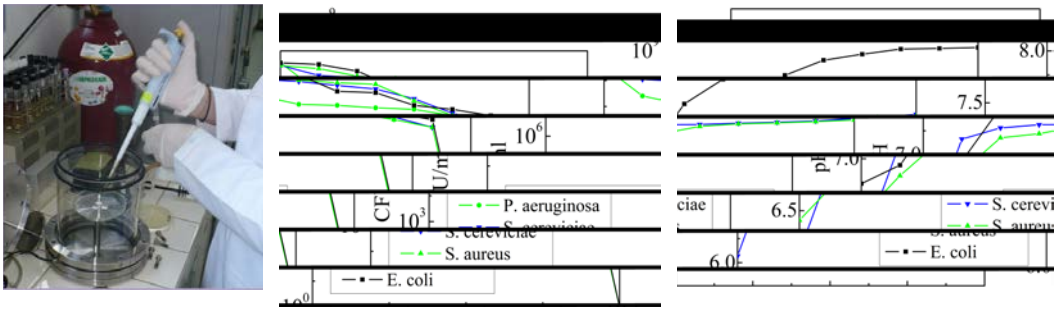

a b c

Figure 12. a) Inoculation in the DBD reactor, b) UFC evolution curves and c) PH evolution survival curves,

The tubes are shaken again and their pH is measured by means of a potentiometer previously calibrated on a control non inoculated 0.75% glucose and red phenol solution. The outcome is displayed in figure 12c implying that the pH level is a function of the metabolic activity in the CFU of the bacterial strands. After an 80 s plasma treatment the metabolic activity increases to the level of the basal state, i.e., the characteristic of the state of null bacterial activity.

4. SO_2, NO_X and H_2S gas degradation

The unremitting pollution increase of the last decades has led to an enormous environmental unbalance which jeopardises the existence of many natural species. Early studies in the 1970's suggested that a series of then massively produced compounds could be responsible for the destruction of the ozone layer. One such product category, fluorocarbons (CFCs), liberates chlorine which is in turn carried to the stratosphere where it reacts with the ozone to depletion [37]. Compounds contributing to the greenhouse effect which accumulate in the troposphere include carbon dioxide (CO_2), methane (CH_4), nitrose oxide (N_2O), sulphur hexafloride (SF_6), clorofluorocarbons (CFC), hydroclorofluorocarbons (HCFC), sulphur dioxide (SO_2), nitrogen oxides (NO_X), carbon monoxide (CO), volatile organic compounds (VOC), ammonia (NH_3) and hydrogen sulphide (H_2S), most of them being the result of industrial processes [38]. In particular, CO_2, SO_2 and NO_X are responsible for the acid rain phenomenon. Chemical and mechanical methods have been devised in order to prevent or, at least, diminish the presence of such compounds. The car industry has introduced the catalytic converter and low sulphur fuels have been developed. The control of bad odours implies unitary operations of separation, filtering and aeration. Odour masking is also practised by spraying inorganic compounds such as zeolites, carbonates or salts [39] including hydrated aluminosilicates of sodium, potassium, calcium, magnesium, aluminium and activated carbon cations. Less conventional techniques involve the use of cold plasmas where gas molecules are converted into non toxic molecules by means of chemical reactions with the active species created by the plasma formation itself [39]. In contrast with thermal plasma temperatures ~10^4 K, cold plasmas exist at practically room temperatures (~298 K) and yet, they present high efficacy in the degradation of toxic compounds although not necessarily from an energy point of view [40]. Thus, additional compounds have been added to the process [41], high power systems have been re-designed [42], electrodes have been modified [43] and catalysis has been specifically developed.

Cold plasmas have been actively studied at ININ-LFP with an emphasis on corona discharges applied to the treatment of gases such as SO_2 and on DBD degradation of nitrogen oxides (NO_X), and hydrogen sulphide (H_2S). In the latter case, both natural (extracted from liquids and sediments at the pollution source) and synthetic (artificially compounded at the laboratory) mixtures have been successfully treated. This has been achieved on the basis of specific models of the chemical kinetics which take into consideration all the main chemical processes of species formation and decomposition.

4.1 Plasma chemistry

The earth's troposphere can act as a natural filter or reactor where several processes of pollutant degradation are carried out. However, the high volume of contaminants entails

negative consequences like ozone losses. The same degradation processes can be carried out in controlled laboratory conditions by means of a cold plasma source, accelerating the chemical processes involved and limiting the creation of environmental hazardous by products. To this purpose, a series of chemical reactions have been induced by a high voltage discharge in a plasma reactor (figure 13). The electric potential accelerates free electrons which collide with gas atoms and molecules, exciting them at first and eventually dissociating them whereby new electrons are delivered. Later on, atoms and electrons collide producing more ions, electrons and, particularly, free radicals capable of degrading toxic molecules through recombination or dissociation.

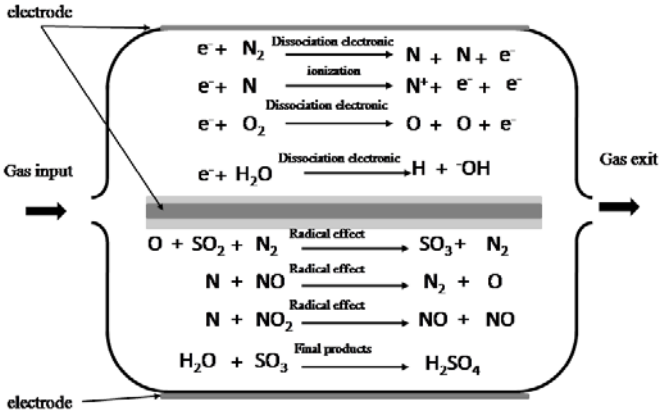

Figure 13. Some events taking place inside the reactor

Controlling the particle temperatures, densities, flows and, therefore, the resulting chemical reactions, demands a careful modulation of several operation parameters such as voltage amplitude, frequency, gas flow and composition, internal pressure, electrode characteristics, reactor temperature and geometry, etc.

4.2 Experimental set up

As mentioned above, cold plasma has been produced at ININ-LFP by means of pulsed corona [27] and DBD [44] discharges. Figure 14 shows the main elements of the experimental array intended for toxic compound degradation. Several reactors have been tested, namely, rectangular, circular, cylindrical and their variants, yielding relevant results [45]. The current version of the cylindrical reactor is constituted by a Pyrex tube concentric to a central stainless steel rod, 3 mm in diameter, playing the role of inner electrode. The dielectric 1 mm Pyrex tube, 11 mm in external diameter and 350 mm long, is wrapped in a copper mesh acting as external electrode allowing a 20 cm^3 effective discharge volume.

4.3 SO_2 degradation

The pulsed corona discharge has been applied to 50-200 μmol/mol SO_2 concentrations diluted in nitrogen, with the addition of oxygen with oxidation purposes. A constant 1 L/min flow of this mixture was maintained implying a ~1.2 s residence time. The reaction was enhanced by the addition of <1% humidity. High voltage 25 kV pulses were applied at 500 HZ to the inner electrode with variable 10-20 μs pulse width as a function of the applied voltage.

The chemical diagnosis of the degradation process has been carried out on a Sensonic 2000 gas analyser. The results from several concentrations are displayed in figure 15. The dilution of the N_2 mixture produces no significant effects on the degradation (figures 15a and 15b) with a similar tendency in all the studied N_2 cases. Figures 15a and 15c show the reproducibility of the process in the presence of 100% N2. The degradation of SO_2 (figure 15d) started with the dilution in O_2, the efficacy of the process increasing along the oxygen content. In general, the addition of humidity enhanced the SO_2 removal, albeit at a slightly higher power consumption. As the humidity percentage was further increased, the removal efficacy declined whereas the power consumption kept on the increase, thus, optimal results were obtained at ~0.5% H_2O.

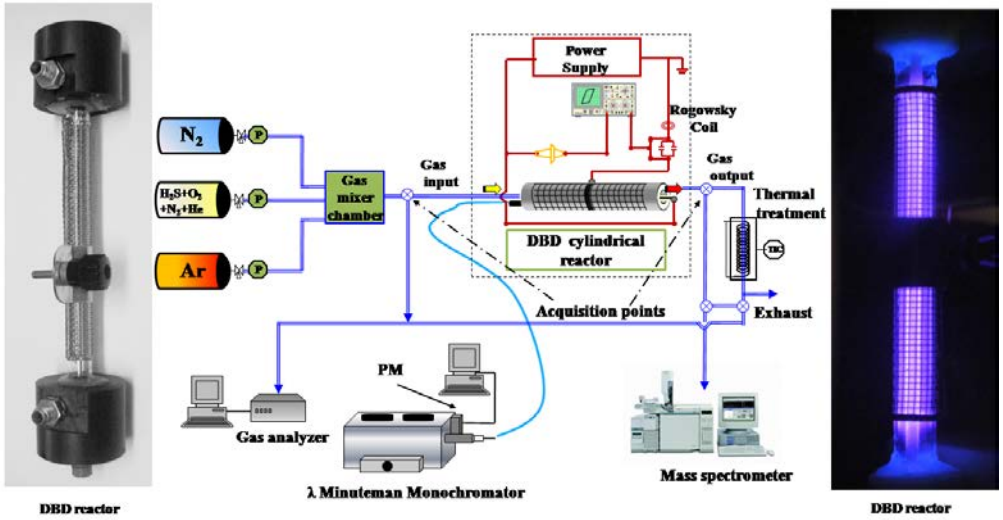

Figure 14. Experimental array for toxic compound degradation

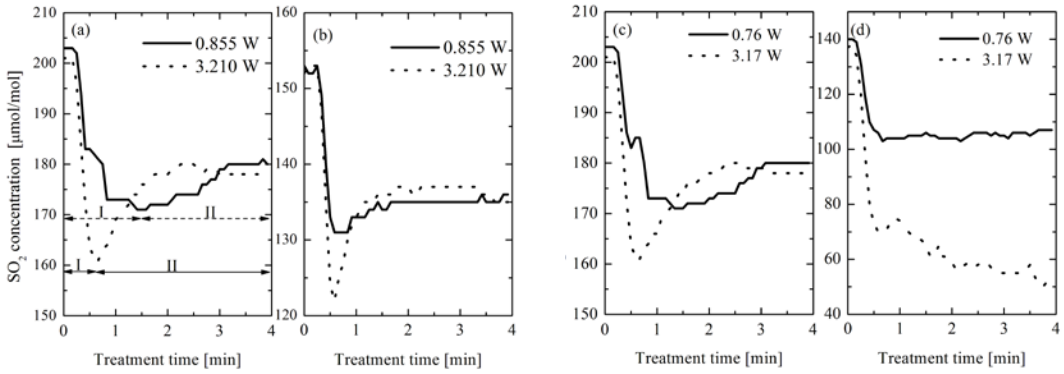

Figure 15. Experimental SO_2 degradation: (a) ~200 μmol/mol SO_2 in 100% N_2, (b) ~150 μmol/mol SO_2 in 100% N_2, (c) ~200 μmol/mol SO_2 in 100% N_2 and (d) ~140 μmol/mol SO_2 in 75%N_2, 25%O_2

4.4 NO_X degradation

The same cylindrical reactor described in section 4.2 was applied to NO_X removal experimentation at ININ-LFP with the exception of the internal electrode which was substituted with a copper filament encapsulated in ceramic in the way of a second dielectric. Thus, the reactor was supplied by a quasi-sinusoidal high voltage source [46] operating up to 25 kVpp at 1.25 kHz, 1.75 kHz and 2.50 kHz, intended for DBD discharges. The gas concentrations ranged from 30 to 200 μmol/mol of NO in N_2. The process did not require the addition of humidity and was conducted in the presence of nitrogen, exclusively. The results show that the power consumption effect is more noticeable at low NO concentrations (figure 16a) than otherwise (figure 16b) all this at a 1.25 kHz frequency. According to the gas selection, there exists a favourable trend to the formation of N_2 and O_2, although a fraction NO is oxidised to NO_2 (figures 16a, 16b).

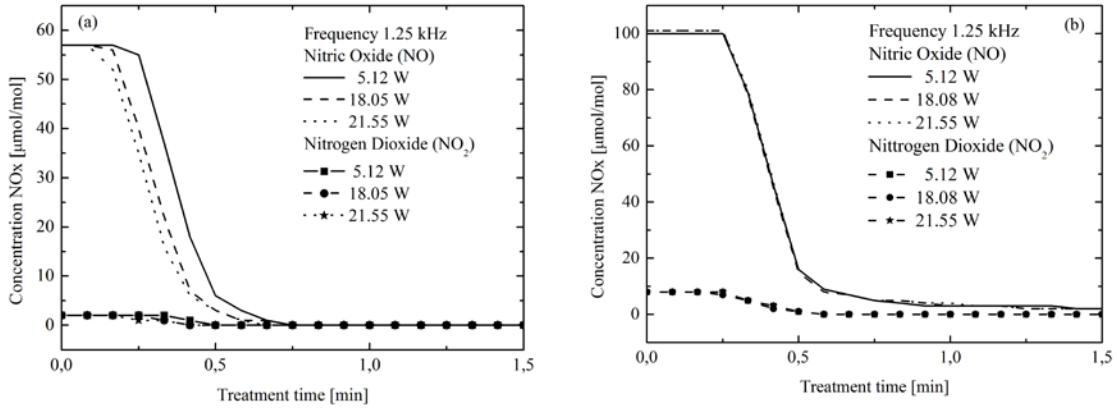

Figure 16. NO_X concentration in a DBD at 1.25 kHz with: (a) 58 μmol/mol and (b) 100 μmol/mol of NO.

4.5 H_2S degradation

Apart from its toxic properties, hydrogen sulphide is recognised by its unpleasant odour, characteristic of residual water bodies such as the Lerma River near Toluca, Mexico, which motivates its removal. This pollution originates in the dumping of industrial (e.g. textile dyes and paints) as well as domestic residual water with high sulphur content under the effects of high temperature and pH changes, delivering H_2S and by hazardous products such as mercaptanes.

The experimentation at ININ-PFL was conducted on a synthetic gas mixture of 100 μmol/mol H_2S diluted in nitrogen, commercially elaborated under quality control norms, resulting in degradation efficiencies <50%, as seen in figure 17a. Then, an increase of this percentage is achieved by the addition of oxygen to the mixture (figure 17b). The efficiency values, as a function of the oxygen content and the power supply, is presented in figure 17c.

5. Conclusions and perspectives

Plasma technology applied to materials science, medicine and ecology is a priority research topic pursued in laboratories throughout the world. The incidental activities at ININ-LFP have contributed significantly since 2002 to this international effort, as follows from its list

of publications in, and constant refereeing of, specialised international journals on plasma, vacuum and electronics. The ININ-LFP group has developed an infrastructure which enables to reach relevant new knowledge in these areas at scientific, technologic and academic levels. In the latter respect, both BA and graduate theses are continuously accomplished with the consequent benefits for the creation of highly trained human resources. The perspectives of the ININ-LFP group involve the consolidation of its current research trends and the development of further plasma applications such as surgical material processing, live skin treatment and tissue cauterisation.

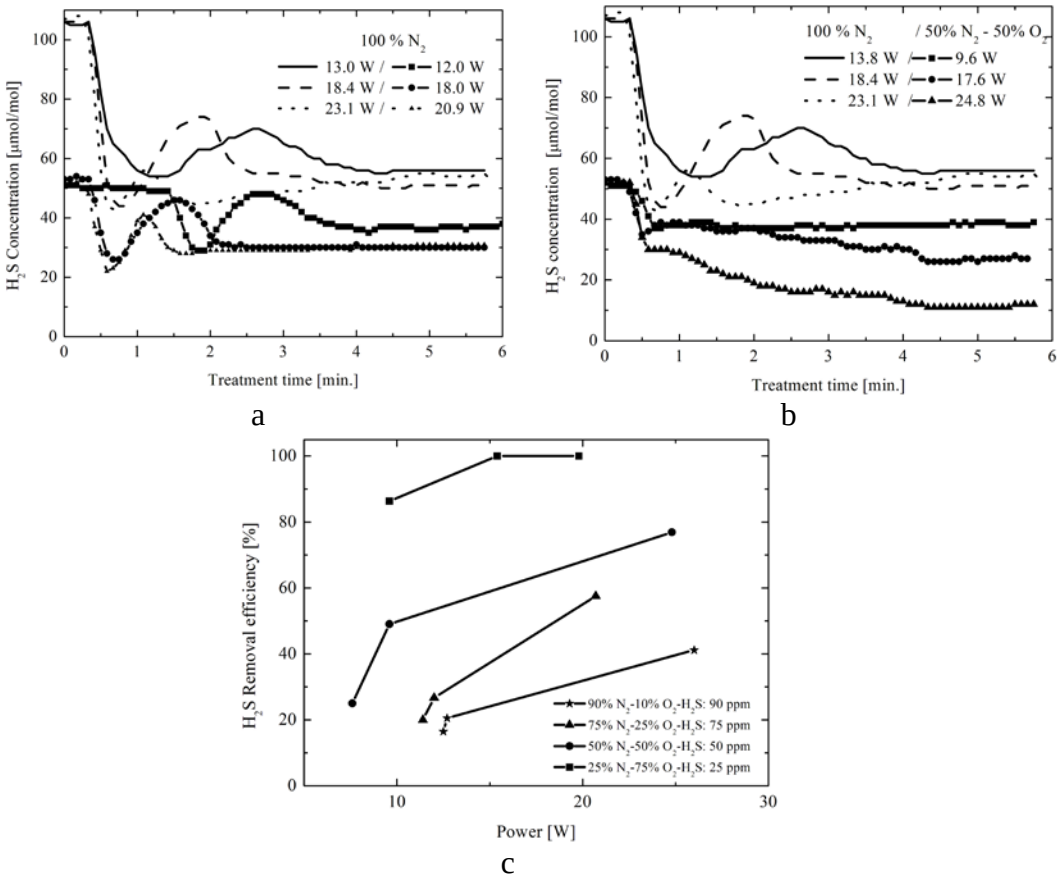

Figure 17. H_2S concentration evolution in (a) 100% N_2; (b) 50%N_2-50% O_2; (c) H_2S degradation efficiency as a function of the N_2-O_2 proportion and the consumed power.

Acknowledgements

The authors are much obliged to their ININ fellow workers for constant support, among others, Dr. Manuel Eduardo Espinoza Pesqueira, Dr. Enrique Camps Carvajal, Dr. Luis Escobar Alarcón, David Alcántara Díaz, Claudio Fernández Ortega, Leticia Carapia Morales, Eleuterio Flores Jiménez and Jorge Pérez del Prado. The authors are equally thankful to the Guadalajara University research team, especially Dr. Josué R. Solís Pacheco and Dr. Blanca R. Aguilar Uscanga as well as the ININ graduate students: Dr. Everardo Efrén Granda Gutiérrez, Dr. Allan Antonio Flores Fuentes, Alejandro Rojas Olmedo, Iván Osvaldo Rossano Díaz, José Arturo Pérez Martínez, Mariana Flores Moreno, Bethsabet

Jaramillo Sierra, Alma Neli Hernández Arias, Hannali Millán Flores and Elizabeth García Alcantara for their talented contributions. Last but not least, the authors are thankful to the ININ-LPF technical staff: María Teresa Torres Martínez, Pedro Ángeles Espinoza e Isaías Santiago Contreras Villa whose dedication and expertise make possible our daily work.

References

1. Conrad JR, Dodd RA, Worzala FJ, Qiu X. Plasma source ion implantation: a new cost-effective, non-line-of-sight technique for ion implantation of materials. Surface and Coatings Technology 36-3/4, 927-937, 1988.
2. López-Callejas R, Muñoz-Castro AE, Valencia R, Barocio SR, Granda-Gutiérrez EE, Godoy-Cabrera OG, Mercado-Cabrera A, Peña-Eguiluz R, de la Piedad-Beneitez A. Surface modification of stainless steel drills using plasma–immersion nitrogen ion implantation. Vacuum 81, 1385-1388, 2007.
3. Valencia-Alvarado R, de la Piedad-Beneitez A, de la Rosa-Vázquez J, López-Callejas R, Barocio SR, Godoy-Cabrera OG, Mercado-Cabrera A, Peña-Eguiluz R, Muñoz-Castro AE. γN-shifting as a function of N2 content in AISI 304 nitriding. Vacuum 81, 1434-1438, 2007.
4. De la Piedad-Beneitez A, Valencia-Alvarado R, López-Callejas R, Barocio SR, Mercado-Cabrera A, Peña-Eguiluz R, Muñoz-Castro AE, Granda-Gutiérrez EE, Rodríguez-Méndez BG, Pérez-Martínez JA, Flores-Fuentes AA. Inductive plasma source for the ion treatment of AISI-304 SS. Physica Scripta T131, 014019, 2008.
5. López-Callejas R, Valencia-Alvarado R, Muñoz-Castro AE, Barocio SR, Mercado-Cabrera A, Peña-Eguiluz R, Granda Gutiérrez EE, de la Piedad-Beneitez A. Enhancement of wear and corrosion resistance of nitrogen implanted dental tools. Vacuum 82, 1350-1352, 2008.
6. Mändl S, Krause D, Thorwarth G, Sader R, Zeilhofer F, Horch HH, Rauschenbach B. Plasma immersion ion implantation treatment of medical implants. Surface and Coatings Technology 142-144, 1046-1050, 2001.
7. Mändl S, Rauschenbach B. Improving the biocompatibility of medical implants with plasma immersion ion implantation. Surface and Coatings Technology 156-1/3, 276-283, 2002.
8. Tian X, Gong C, Yang S, Luo Z, King-Yu FR, Chu PK. Oxygen Plasma Ion Implantation of Biomedical Titanium Alloy. IEEE Trans. Plasma Science 34-4, 1235-1240, 2006.
9. Chu PK. Plasma. Treated Biomaterials. IEEE Trans. Plasma Science 35-2, 181-187, 2007.
10. Byung-Dong H, Jung-Min L, Dong-Soo P, Jong-Jin Ch, Jungho R, Woon-Ha Y, Byoung-Kuk L, Du-Sik S, Hyoun-Ee K, Mechanical and in vitro biological performances of hydroxyapatite–carbon nanotube composite coatings deposited on Ti by aerosol deposition Acta Biomaterialia 5-8, 2821-3280, 2009.
11. Hoene A, Walschus U, Patrzyk M, Finke B, Lucke S, Nebe B, Schroeder K, Ohl A, Schlosser M. In vivo investigation of the inflammatory response against allylamine plasma polymer coated titanium implants in a rat model, Acta Biomaterialia. Article in press, accepted manuscript (2009).
12. Askeland DR, Phulé PP. The Science and Engineering of Materials. 4th Edition, Thomson-Engineering, 2002.

13. Oshida Y. Bioscience and bioengineering of titanium materials. UK: Elsevier BV, 2007.
14. Wang ML, Tuli R, Manner PA, Sharkey PF, Hall DJ, Tuan RS. Direct and indirect induction of apoptosis in human mesenchymal stem cells in response to titanium particles. Journal of Orthopedic Research 21-4, 697-707, 2003.
15. Granda-Gutiérrez EE, Millán-Flores H, López-Callejas R, Muñoz-Castro AE, Valencia R, Peña-Eguiluz R, Mercado-Cabrera A, Barocio SR, de la Piedad-Beneitez A, Superficial characterization of a TiO2–TiN0.26 layer implanted in titanium. Superficies y Vacío 20-3, 11-16, 2007.
16. Valencia-Alvarado R, de la Piedad-Beneitez A, de la Rosa-Vázquez J, López-Callejas R, Barocio SR, Godoy-Cabrera OG, Mercado-Cabrera A, Peña-Eguiluz R, Muñoz-Castro AE. Nitriding of AISI 304 stainless steel in a 85% H2/15% N2 mixture with an inductively coupled plasma source, Vacuum 82, 1360-1363, 2008.
17. Muñoz-Castro AE, López-Callejas R, Granda-Gutiérrez EE, Valencia R., Barocio SR, Peña-Eguiluz R, Mercado-Cabrera A, de la Piedad-Beneitez A. Ion implantation of oxygen and nitrogen in CpTi. Progress in Organic Coatings 64, 259-263, 2009.
18. Valencia-Alvarado R, de la Piedad-Beneitez A, López-Callejas R, Barocio SR, Mercado-Cabrera A, Peña-Eguiluz R, Muñoz-Castro AE, de la Rosa-Vázquez J. Oxygen implantation and diffusion in pure titanium by an rf inductively coupled plasma. Vacuum 83, S264-S267, 2009.
19. Granda-Gutiérrez EE, López-Callejas R, Peña-Eguiluz R, Mercado-Cabrera A, Muñoz-Castro AE, Valencia R, Barocio SR, de la Piedad-Beneitez A, Millán-Flores H, N-O Mix Optimisation in Low Energy Dense DC Glow Surface Ti Conditioning. European Physical Journal D. 54, 281-286, 2009.
20. López-Callejas R, H. Millán-Flores, A. E. Muñoz-Castro; R. Valencia-Alvarado, A. Mercado-Cabrera, R. Peña Eguiluz, S. R. Barocio and A. de la Piedad Beneitez, "Nitriding of 6061T6 aluminium by plasma immersion ion implantation at low energy", Aceptado para ser publicado en la revista Progress in Organic Coatings.
21. Pokryvailo A, Yankelevich Y, Wolf M, Abramzon E, Wald S, Welleman A. A high-power pulsed corona source for pollution control applications. IEEE Trans. Plasma Sci 32-5/1, 2045-2054, 2004.
22. Katsuki S, Akiyama H, Abou-Ghazala A, Schoenbach KH. Parallel streamer discharges between wire and plane electrodes in water. IEEE Trans. Dielectr. Electr. Insul 9-4, 498-506, 2002.
23. Efremov NM, Adamiak BY, Blochin VI, Dadashev SJ, Dmitriev KI, Semjonov VN, Levashov VF, Jusbashev VF. Experimental investigation of the action of pulsed electrical discharges in liquids on biological objects. IEEE Trans. Plasma Sci 28-1, 224-229, 2000.
24. Kogelschatz U. Dielectric-barrier Discharges: their history, discharge physics, and industrial applications. Plasma Chemistry and Plasma Processing 23-1, 1-46, 2003.
25. Rodríguez-Méndez BG, López-Callejas R, Peña-Eguiluz R, Mercado-Cabrera A, Valencia R, Barocio SR, de la Piedad-Beneitez A, Benítez-Read JS, Pacheco-Sotelo JO. A simulation of pre-arcing plasma discharge processes in water purification. American Institute of Physics CP875, 266-269, 2006.
26. Rodríguez-Méndez BG, Mercado-Cabrera A, López-Callejas R, Peña-Eguiluz R, Valencia-Alvarado R, Barocio SR, de la Piedad-Beneitez A, Benítez-Read JS,

Pacheco-Sotelo JO. AOP in water by means of a DBD conducted in a coaxial reactor, Journal of Advanced Oxidation Technologies 11-1, 84-90, 2008.
27. Rodríguez-Méndez BG, López-Callejas R, Peña-Eguiluz R, Mercado-Cabrera A, Valencia R, Barocio SR, de la Piedad-Beneitez A, Benítez-Read JS, Pacheco-Sotelo JO. Instrumentation for pulsed corona discharge generation applied to water. IEEE Trans. Plasma Science 36-1, 185-191, 2008.
28. Anpilov AM, Barkhudarov ÉM, Kop'ev VA, Kossy IA, Silakov VP. Atmospheric electric discharge into water. Plasma Physics Reports 32-11, 968-972, 2006.29.
29. Menashi W.P., Treatment of surfaces, U.S. Patent No. 3,338,163, May 14, 1968.
30. Moisan M, Barbeau J, Crevier MCh, Pelletier J, Philip N, Saoudi B. Plasma sterilization, methods and mechanisms. Pure Appl. Chem. 74, 349-358, 2002.
31. Roth JR, Nourgostar S, Bonds TA. The one atmosphere uniform glow discharge plasma a platform technology for the 21st Century, IEEE Trans. Plasma Sci., 35, 233-250, 2007.
32. Moreau M, Orange N, Feuilloley MGJ. Non-thermal plasma technologies: New tools for bio-decontamination, Biotechnology Advances 26, 610-617, 2008.
33. Pérez-Martínez JA, Peña-Eguiluz R, López-Callejas R, Mercado-Cabrera A, Valencia-Alvarado R, Barocio SR, de la Piedad-Beneitez A. Power supply for plasma torches based on a class-E amplifier configuration. Plasma Process Polym 5, 593-598, 2008.
34. Pérez-Martínez JA, Peña-Eguiluz R, López-Callejas R, Mercado-Cabrera A, Valencia-Alvarado R, Barocio SR, Godoy-Cabrera OG, de la Piedad-Beneitez A. Benítez-Read JS, Pacheco-Sotelo JO. Electrical characterization of an RF glow discharge at room pressure, AIP Plasma and Fusion Science CP875, 250-253, 2006.
35. Pérez-Martínez JA, Peña-Eguiluz R, López-Callejas R, Mercado-Cabrera A, Benítez-Read JS, Pacheco-Sotelo JO. Valencia R, Barocio SR. An RF microplasma facility development for medical applications. Surf. Coat. Tech. 201, 5684-5687, 2007.
36. R. Peña-Eguiluz, J. A. Pérez-Martínez, J. Solís-Pacheco, B. Aguilar-Uscanga, R. López-Callejas, A. Mercado-Cabrera, R. Valencia-Alvarado, A. E. Muñoz-Castro, S. R. Barocio, and A. de la Piedad Beneitez. Instrumentation for a plasma needle applied to E. coli bacteria elimination. European Physical Journal-Applied Physics 49 (2010).
37. Molina MJ. Polar ozone depletion. Nobel Lecture 8, 250-263, 1995.
38. McAdams R. Prospects for non-thermal atmospheric plasmas for pollution abatement J. Phys. D Appl. Phys. 34, 2810-2821, 2001.
39. Zhang Q, Feddes J, Edeogu I, Nyachoti M, House J, Small D, Liu C, Mann D, Clark G. Odour production, evaluation and control. Project MLMMI 02-HERS-03 Final Report Submitted to Manitoba Livestock Manure Management Initiative Inc. October, 2002.
40. Bai Y, Chen J, Li X, Zhang Ch. Non-thermal plasmas chemistry as a tool for environmental pollutants abatement. Reviews of Environmental Contamination and Toxicology 201, 117-136, 2009.
41. Ken Y, Kensuke K, Takashi H, Hiroshi M, Shinji K, Hiroshi M, Toru Y. Efficient decomposition of NO by ammonia radical-injection method using an intermittent dielectric barrier discharge. Thin Solid Films 515-9, 4278–4282, 2007.
42. Yankelevich Y, Pokryvailo A. High-power short-pulsed corona: investigation of electrical performance, SO_2 removal, and ozone generation. IEEE Trans. Plasma Sci 30-5, 975–1981, 2002.

43. Harada N, Moriya T, Matsuyama T, Yamamoto H, Hosokawa S. A novel design of electrodes system for gas treatment integrating ceramic filter and SPCP method. Journal of Electrostatics, 65, 37–42, 2007.
44. Godoy-Cabrera O, Benítez-Read J, López-Callejas R, Pacheco-Sotelo J. A high voltage resonant inverter for dielectric discharge barrier cell plasma applications. Int. J. Electronics, 87, 361-376, 2000.
45. Flores-Moreno M, Mercado-Cabrera A, Valencia-Alvarado R, López-Callejas R, Barocio DS, Peña Eguiluz R, Muñoz-Castro A, Jaramillo SB. NOx Chemical Reduction in a Cylindrical DBD Reactor: Theoretical and experimental analysis. International Journal of Plasma Environmental Science Technology IJPEST, 3-108, 43-48, 2009.
46. Mercado-Cabrera A, López-Callejas R, Pacheco-Pacheco M, Valencia-Alvarado R, León del Villar E, Barocio S. R, Peña-Eguiluz R, Muñoz-Castro A. Jerks-and-jumps type electrode diagnostics in a DBD reactor by OES. Laser Physics, 18, 292-297, 2008.